To appear in Proceedings of SAMPE 2007. Baltimore, MD. 3-7 June 2007.

HYPODERMIC NEEDLE PUNCTURE OF SHEAR THICKENING FLUID (STF)-TREATED FABRICS

J. M. Houghton,[1] B. A. Schiffman,[1] D. P. Kalman,[1] E. D. Wetzel,[2] and N. J. Wagner[1]

[1]Department of Chemical Engineering and Center for Composite Materials,
University of Delaware, Newark, DE 19716

[2]U.S. Army Research Laboratory
Aberdeen Proving Ground, MD 21005

ABSTRACT

Shear thickening fluids (STF) are flowable at low shear rates but become macroscopically rigid at high shear rates. Previous studies have shown that STF-treated fabrics exhibit high penetration resistance under spike, stab, and low velocity ballistic threats. In this study, the resistance of STF-fabrics to needle puncture is explored. Factors controlling fabric resistance to needle puncture include needle diameter, fabric type, and the presence of the STF treatment. Multi-layer fabric specimens were placed on a foam backing and slowly loaded by hypodermic needles oriented normal to the specimen face. Load versus displacement was recorded, with fabrics of higher puncture resistance exhibiting higher peak loads before breakthrough. A range of needle sizes, needle types, fabric types, and treatments were tested. The loading data shows behavior characteristic of previous theoretical predictions for fabric puncture. The results illustrate important interactions between needle size, fabric architecture, and treatments, with STF application providing important improvements in puncture resistance under many conditions.

KEY WORDS: Armor Technology, Materials - Fabric/Textile Reinforcement

1. INTRODUCTION

Law enforcement officers face a significant risk when conducting personal searches due to the widespread use of hypodermic needles. During searches, these officers often must reach into unknown areas that may contain new or used needles. In addition to direct puncture wounds, these needles can carry dangerous and infectious diseases. Similar risks exist for medical employees, veterinarians, and sanitation workers who come into contact with used hypodermic needles. For these applications, protective materials that prevent hypodermic needle puncture are needed. Because of the particular risk to hands and fingers, these protective materials should be thin and flexible so that they can be integrated into gloves.

Stab threats can be classified into two categories: puncture and cut. Puncture refers to penetration by instruments with sharp tips but no cutting edge, such as ice picks or awls. Cut refers to contact with knives with a continuous cutting edge. Cut threats are generally more difficult to stop than puncture, since the long cutting edge presents a continuous source of damage initiation during the stab event. Hypodermic needles fall into both of these categories,

with thin sharp tips and a beveled cutting edge. Previous studies have shown that hypodermic needles require less force to penetrate woven fabrics than standard needles (Leslie et al, 1995).

Many commercial products exist that offer resistance to hypodermic needle threats. One approach is to construct a high yarn count fabric. These tightly woven fabrics defeat puncture threats by repressing "windowing" mechanisms, in which the yarns spread apart to allow foreign object penetration between yarns without significant fiber fracture. Examples of this approach are TurtleSkin™ fabric developed by Warwick Mills, Inc. (New Ipswich, NH), and Kevlar® Correctional™ developed by DuPont (Richmond, VA). A different approach is to layer an array of hard platelets onto a fabric support, providing a rigid barrier to penetration on a globally flexible substrate. One such commercial product is SuperFabric® developed by HDM, Inc. (Oakdale, MN), in which hard platelets composed of a proprietary ceramic-polymer composite are arrayed on a flexible fabric backing.

Shear thickening is a non-Newtonian flow behavior observed as an increase in viscosity with increasing shear rate or applied stress (Barnes, 1989; Maranzano and Wagner, 2001; Lee and Wagner, 2003). Concentrated colloidal suspensions consisting of solid particles dispersed in a liquid medium have been shown to exhibit reversible shear thickening resulting in large, sometimes discontinuous increases in viscosity above a critical shear rate. This transition from a flowing liquid to a solid-like material is due to the formation of shear induced transient aggregates, or "hydroclusters," that dramatically increase the viscosity of the fluid. Support for this hydrocluster mechanism has been demonstrated experimentally through rheological, rheo-optics and flow-SANS experiments (Bender and Wagner, 1995; Maranzano and Wagner, 2002), as well as computer simulation (Bossis and Brady, 1989; Catherall et al., 2000)

Previous studies have investigated the ballistic (Decker et al., 2005; Lee et al., 2002, 2003), and stab (Decker et al., 2007) properties of woven aramid fabrics impregnated with a colloidal, discontinuous shear thickening fluid (STF). These investigations have shown that, under some conditions, this STF-fabric composite offers ballistic and stab properties that are superior to neat (non-impregnated) fabrics. Additionally, STF-fabrics were shown to remain thin and flexible like conventional fabrics.

In this paper the resistance of STF-fabrics to hypodermic needle threats is reported. The contributions of needle diameter and fabric type will be characterized and examined mechanistically.

A commonly used method for evaluating the puncture resistance of fabrics is ASTM standard D4833-00e1 (ASTM, 2005). This standard test method initiates puncture at the center of an edge-clamped, 45-mm-diameter area of unbacked fabric. In contrast, in this study the fabrics are unclamped, and backed by a foam witness. The foam witness is assembled according to the National Institute of Justice (NIJ) standard 0115.00 for stab testing of body armor (NIJ, 2000), and is designed to replicate the response of human tissue during impact. We use this foam witness, instead of a clamped fabric, to better simulate fabric-tissue interactions.

2. EXPERIMENTAL METHODS

2.1 Materials STFs were prepared by dispersing colloidal silica particles (450 nm average diameter) in 200 M_w polyethylene glycol (PEG, ρ=1.12 g/cm^3, η=0.049 Pa·s) at a mass fraction of 67%, corresponding to an approximate volume fraction of 52%. Rheological measurements show that these STFs demonstrate discontinuous shear thickening at a shear rate of approximately 20 s^{-1}. Comprehensive rheology of such STFs is documented in Lee and Wagner (2002, 2003).

Two types of Kevlar fabric, Hexcel Reinforcements (Anderson, SC) Style 706 and Style 779, were tested (Table 1). Style 706 is a plain weave of 600 denier Kevlar KM-2 yarns with a yarn count of 34 × 34 yarns per inch (1340 × 1340 yarns per meter) with an areal density of 180 g/m^2. Style 779 is a plain weave of 200 denier Kevlar K159 yarns with a yarn count of 70 × 70 yarns per inch (2760 × 2760 yarns per meter) with an areal density of 132 g/m^2.

To fabricate the STF-fabric composites, the STF was first diluted in ethanol at a 3:1 volume ratio of ethanol:STF. Individual fabric layers, each measuring 38.1 cm × 38.1 cm, were then soaked in the solution for one minute, squeezed to remove excess fluid, and dried at 60°C for 30 minutes. This drying process removes the ethanol co-solvent, and leaves behind STF in the fabric. This 38.1 cm × 38.1 cm fabric was cut into four equal-sized squares. The mass addition of STF was 20.2% for 706, and 15.1% for 779 (Table 1).

In all cases, puncture targets consist of four layers of Kevlar. Table 1 lists the areal density and thickness of these four-layer targets. Thickness was measured using a micrometer. Note that the areal densities of the targets are not equal. However, for needle puncture applications such as gloves, thinness and flexibility are more important than weight. The target thicknesses are much thinner than previous reported puncture and stab results for STF-fabrics (Decker et al., 2007), although there is some variation in total target thickness. A follow-on study is underway to compare targets of carefully matched total thickness.

2.2 Quasistatic needle testing Six different hypodermic needles were tested, from 12-22 gauge (Table 2) (Contran Corp., Portsmouth, RI). Figure 1 shows the size of the needles relative to the 706 and 779 fabrics. Note that 12 gauge needles are commonly used for applications such as implanting pet tracking chips, while 22 gauge needles are commonly used for drawing blood. Figure 1b shows that hypodermic needles are hollow tubes with beveled tips, which present a combination of cutting and puncture mechanisms.

Table 1: Fabric properties.

Label	Yarn material	Yarn count (yarns/in)	Yarn denier	STF wt %	Single layer areal density (g/m^2)	Target areal density (g/m^2)	Target thickness (mm)
Neat 706	Kevlar KM-2	34 X 34	600	0.0%	180	720	0.81
STF-706				20.2%	216	865	1.06
Neat 779	Kevlar K159	70 X 70	200	0.0%	132	528	0.51
STF-779				15.1%	152	608	0.66

Table 2: Needle geometries used for quasistatic puncture testing.

Gauge	Nominal I.D. (mm)	Nominal O.D. (mm)
12	2.16	2.77
14	1.60	2.11
16	1.19	1.65
18	0.838	1.27
20	0.584	0.902
22	0.394	0.711

The stab targets are placed on a multi-layer foam backing, based on the NIJ stab standard (NIJ, 2000). This backing consists of four layers of 5-mm-thick neoprene sponge, followed by one layer of 31-mm-thick polyethylene foam (all backing materials from PCF Foam Corp., Cincinnati, OH). Synthetic polymer-based Polyart™ witness papers (Arjobex Corp., Charlotte, NC) were placed between the target and foam backing, and behind each layer of neoprene sponge (Decker et al., 2007), although the number of witness layers penetrated are not reported in this study.

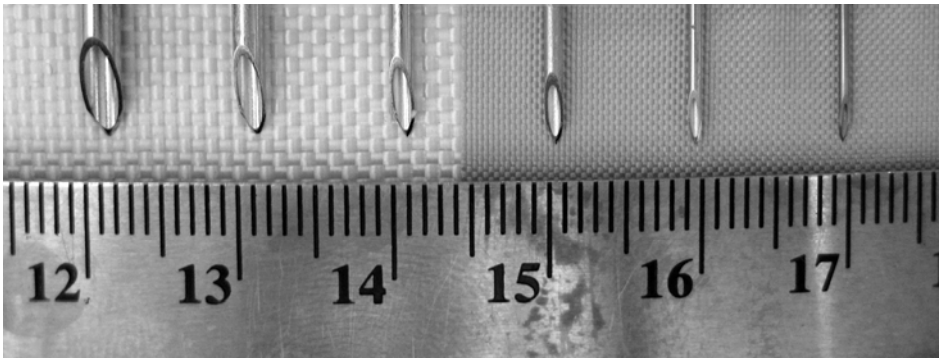

(a)

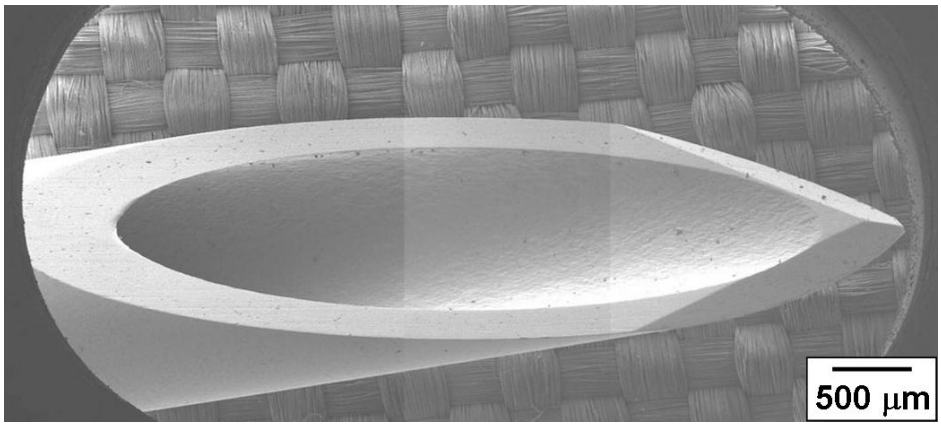

(b)

Figure 1: (a) Hypodermic needles, from left to right, 12, 14, 16, 18, 20, and 22 gauge. Background is neat 706 (left) and 779 (right) fabrics. (b) Composite SEM image of a 16 gauge needle tip. Background is neat 779 fabric.

Needles were rigidly mounted to an Instron 4201 load frame, and were loaded into the targets at a rate of 5 mm/min over a total displacement of 20 mm for all needles except for 22 gauge. Only 10 mm of displacement was used for the 22 gauge needles because their shafts are shorter than 20 mm. For consistency, zero sample displacement is defined as the displacement at which load equals 0.05 N. Five samples were run in all cases, with a new needle used for each fabric target. If a needle bent during testing, the test was repeated with a new needle.

3. RESULTS

Figure 2a shows a typical force versus displacement curve. Needle loading into the foam backing generates a mostly linear force versus displacement curve with small peaks every 5-6 mm. In contrast, needle loading into the fabric targets produces two strong peaks, the first occurring at approximately 5 mm of displacement, and the second occurring at approximately 10 mm of displacement. After the second load peak, the fabric force curves are approximately linear and parallel to the foam backing curve.

The mechanisms of puncture in woven fabrics have been analyzed by Termonia (2004), for the case of a cylindrical penetrator with a conical tip. Although this penetrator is geometrically different from a hypodermic needle, we expect that many of the same basic mechanisms apply to our experiments. Figure 2b illustrates the puncture mechanisms observed for our experiments, which are also labeled on the STF-779 curve of Fig. 2a. The stages of penetration can be summarized as: (i) initial contact, (ii) loading the fabric prior to initial puncture, (iii) initial fabric puncture, resulting in the first peak load and the initiation of fabric windowing and cutting, (iv) increasing loads as needle contact diameter increases, widening the window and cut sizes (v) second peak load, when fabric is cut and windowed to maximum damage zone size, and (vi) relaxation in fabric loads as fabric slides along constant diameter needle shaft.

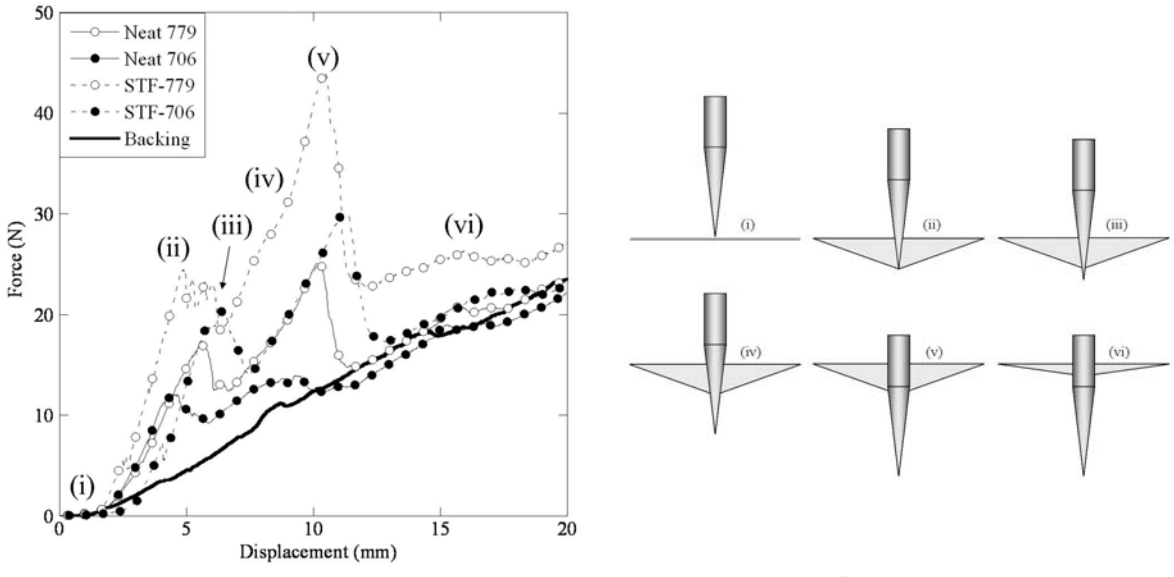

(a) **(b)**

Figure 2: (a) Force versus displacement for 16 gauge needle. (b) Schematic of the needle puncture process (based on Termonia, 2004).

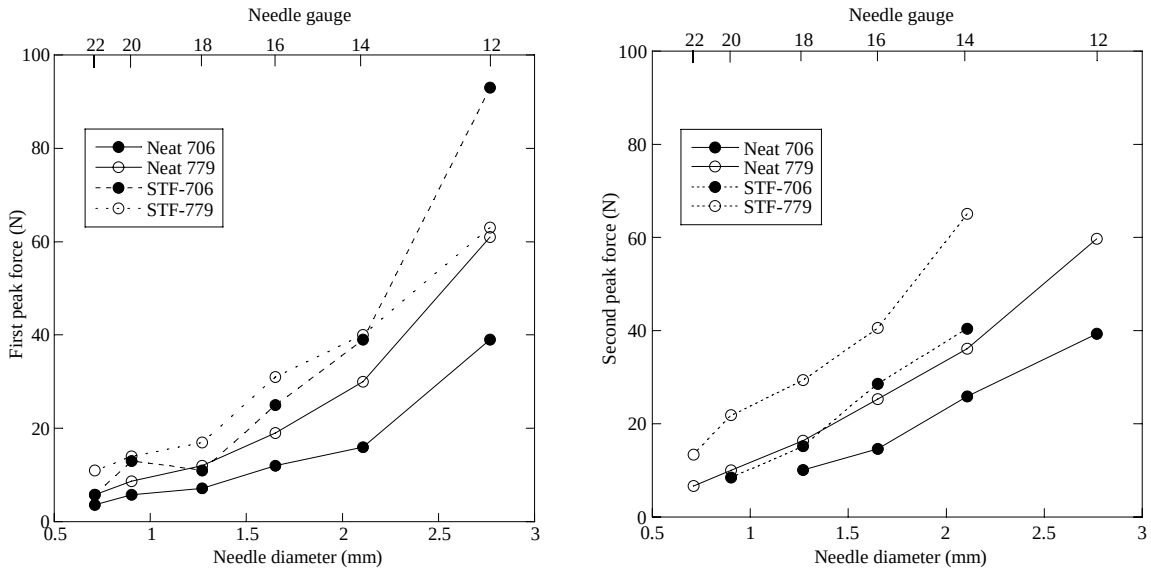

(a) **(b)**

Figure 3: (a) First peak load and (b) second peak load versus needle size.

Our force versus displacement results agree qualitatively with the modeling results of Termonia (2004), if the foam witness loads are subtracted from the total force curve. Both sets of results show a first peak force followed by a drop in force, followed by another peak and then a drop again to a nominal load. Termonia predicts a peak force on the order of 100 N for a 1.4-mm-diameter conical needle penetrating an unbacked Kevlar target with areal density between 100-400 g/m^2. These simulated peak forces are somewhat higher than our measured values, 10-40 N for needles of comparable diameter and targets of ~ 500-1000 g/m^2. The lower peak forces in the present study could be due to the cutting action of the hypodermic needles.

Figure 3 and Table 3 summarize first and second peak forces during quasistatic needle loading, for a number of needle sizes. As needle diameter increases (decreasing gauge) both the first and second peak forces increase. The STF-fabrics perform better when compared to neat fabrics, for all needle gauges except 12 gauge, where STF-779 and Neat 779 perform similarly. Furthermore, 779 fabrics perform better than 706 fabrics for all needles, except 12 gauge. It is also important to note that STF-706 had slightly lower second peak forces than Neat 779 for needle gauges of 20 and 18. All tests had measurable first peak forces. However only 14, 16, and 18 gauge needles produced second peaks for all targets.

Table 3: Peak loads versus needle size.

	Neat 706		**Neat 779**		**STF-706**		**STF-779**	
Needle Gauge	**First peak (N)**	**Second peak (N)**	**First peak (N)**	**Second peak (N)**	**First peak (N)**	**Second peak (N)**	**First peak (N)**	**Second peak (N)**
12	39 ± 4	38 ± 1	61 ± 10	60 ± 9	93 ± 36	-	63 ± 22	-
14	16 ± 2	26 ± 2	30 ± 4	35 ± 2	39 ± 9	41 ± 6	40 ± 6	65 ± 10
16	12 ± 1	15 ± 1	19 ± 1	25 ± 1	25 ± 4	30 ± 1	31 ± 5	40 ± 12
18	7.2 ± 0.5	10 ± 1	12 ± 1	16 ± 2	11 ± 2	15 ± 2	17 ± 3	29 ± 2
20	5.8 ± 0.3	-	8.7 ± 1	11 ± 1	13 ± 7	8.4 ± 0.5	14 ± 3	22 ± 3
22	3.6 ± 0.7	-	5.8 ± 0.5	6.1 ± 1	5.8 ± 1	-	11 ± 1	13 ± 2

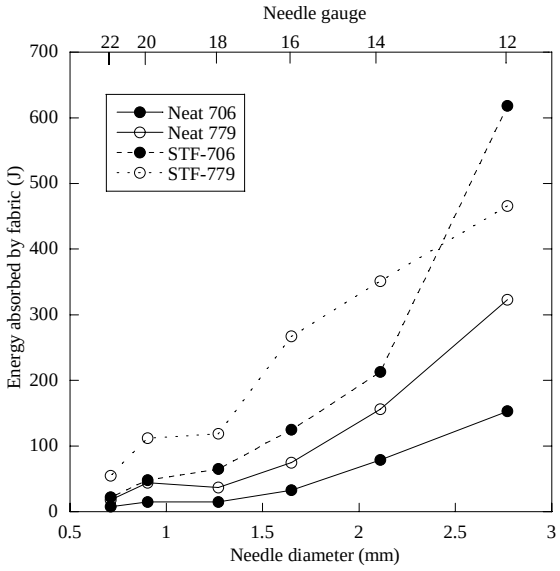

Figure 4: Energy absorbed versus needle size.

We can also quantify total puncture energy by integrating the force versus displacement curve with respect to displacement, and then subtracting the energy contribution from puncture into the foam backing. Foam backing energy absorption values were generated by running five puncture experiments directly into the foam witness, with no target, for each needle gauge. The average energy values for the five experiments are then used as the estimated foam energy values, ranging from 18-340 J for needle sizes of 22-12 gauge, respectively.

Figure 4 and Table 4 show the resulting fabric energy absorption data. The energy absorbed by the fabric increases with increasing needle diameter (decreasing gauge). STF-fabrics performed better than neat fabrics. 779 performed better on all tests than 706 except for 12 gauge needles.

Figure 5 shows the front of the first layer and the back of the last layer of (a) STF-706, (b) STF-779, and (c) neat 779 targets after 16 gauge needle testing. The STF-706 target appears to have significantly less fiber damage than the STF-779 target. The STF-706 target also appears to have more yarn movement (notice the gaps between yarns in the front STF-706 image) allowing windowing and puncture. In contrast, the STF-779 yarns appear stationary and defeated due to cut failure of fibers. The STF-779 target appears to have more fiber damage than the neat 779 target. The lack of an obvious hole in the back of the neat 779 target could indicate that the needle penetrated through windowing, but then the yarns returned to their original positions upon removal of the needle.

Figure 6 shows the front and back of (a) STF-706, and (b) STF-779 after 12 gauge needle testing. Note that again the STF-706 target shows fewer cut yarns and more relative yarn motion, as compared to the STF-779 target. Also note that a C-shaped damage pattern can be seen in both the front images of STF-706 and STF-779, which is caused by the geometry of the hypodermic needle.

Table 4: Energy absorbed versus needle size.

Needle Gauge	Neat 706 (J)	Neat 779 (J)	STF-706 (J)	STF-779 (J)	Backing (J)
12	153 ± 40	323 ± 67	618 ± 121	466 ± 66	338 ± 53
14	79 ± 16	156 ± 18	213 ± 32	351 ± 42	248 ± 23
16	33 ± 10	75 ± 8	125 ± 11	267 ± 21	222 ± 1
18	15 ± 3	37 ± 6	63 ± 8	119 ± 13	174 ± 0
20	15 ± 10	44 ± 16	48 ± 15	112 ± 12	122 ± 11
22	8 ± 4	18 ± 5	22 ± 4	55 ± 8	18 ± 3

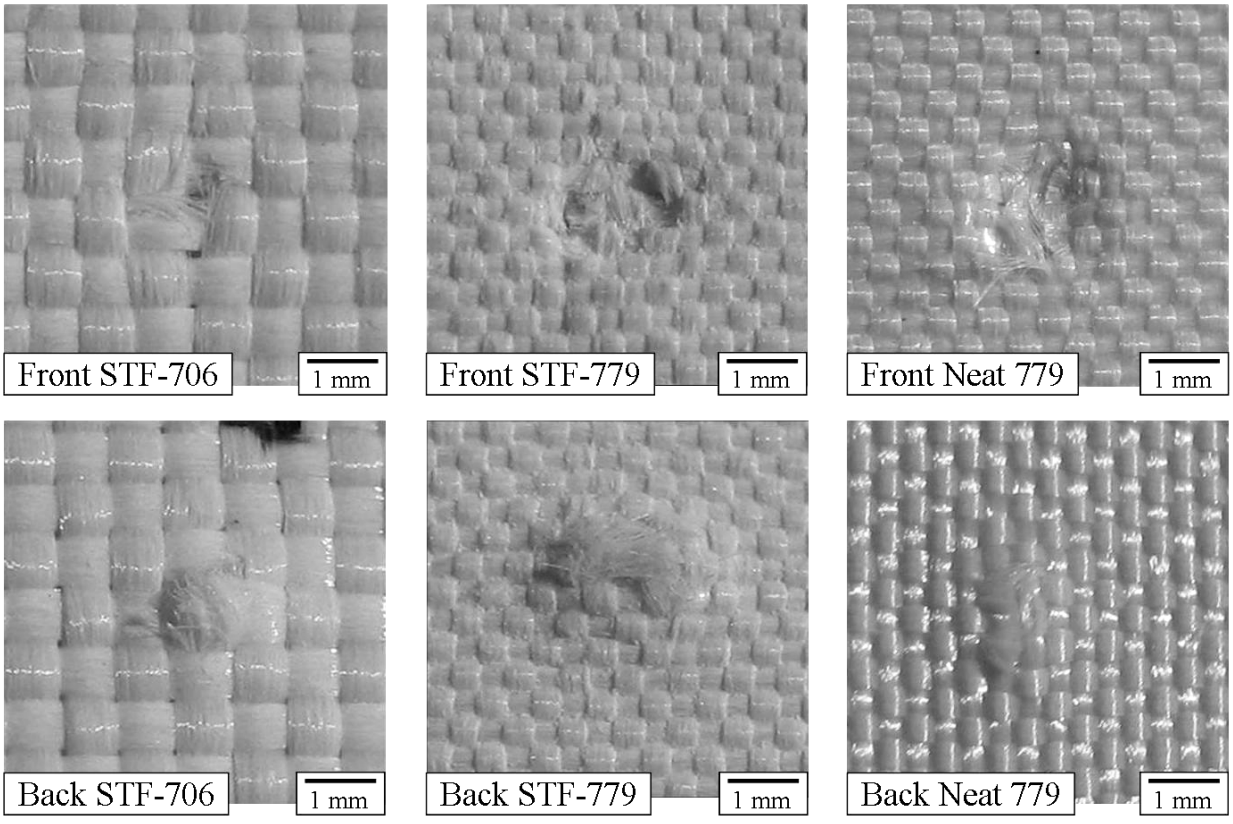

(a) **(b)** **(c)**

Figure 5: Photos of targets after 16 gauge needle testing. (a) STF-706, (b) STF-779, and (c) neat 779.

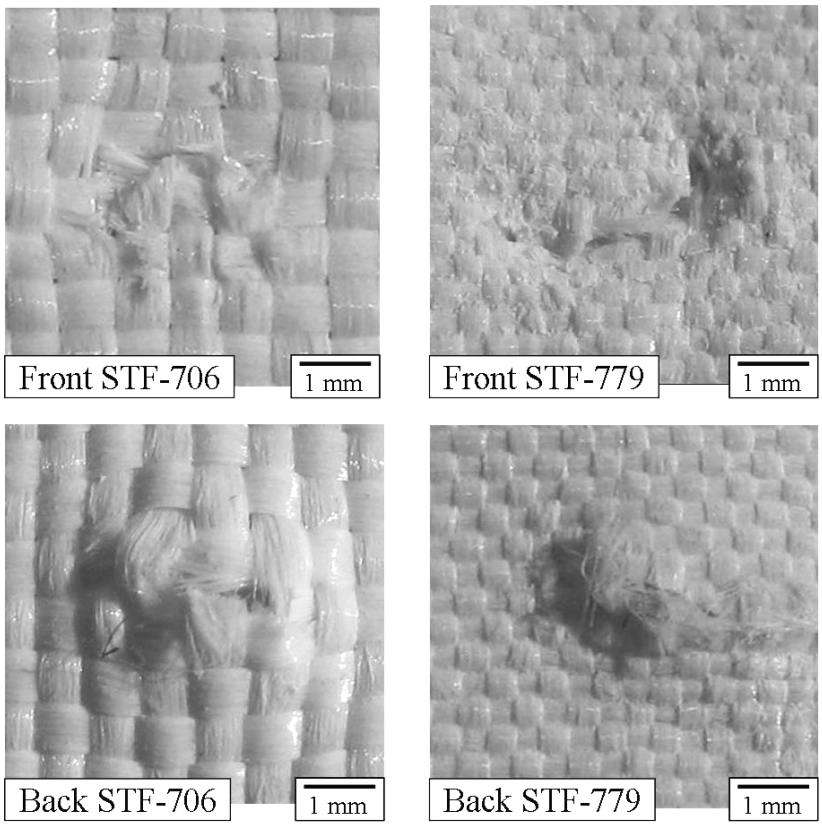

(a) **(b)**

Figure 6: Photos of targets after 12 gauge needle testing. (a) STF-706 and (b) STF-779.

Table 5 shows the number of needles bent for each gauge and fabric. This data gives a very crude estimate of the probability of needle bending, as opposed to penetration, for different fabric and needle combinations. In all cases the needles did not bend along their shaft, but instead merely bent at their tip. Needle bending was only observed for the largest needle (12 gauge), with STF-treated fabrics, and the smallest needles (20 and 22 gauge), for the neat fabrics. Bending of the large needles could be explained by the low probability of windowing for these larger needle sizes, leading to higher overall loads on the needle tip. Bending of the smaller needles could be due to their finer dimensions, which make them more susceptible to bending. However, it is surprising that, for small needles, only neat fabrics caused bent needles. More experiments are needed to verify these trends.

Table 5: Number of bent needles for each needle size and fabric type.

Gauge	Neat 706	Neat 779	STF 706	STF 779
12	0	0	2	1
14	0	0	0	0
16	0	0	0	0
18	0	0	0	0
20	1	0	0	0
22	0	1	0	0

4. DISCUSSION AND CONCLUSIONS

Quasistatic needle testing demonstrates that the addition of STF improves the needle puncture resistance of fabrics, and that STF-779 offers the best needle resistance to all but the largest needle diameters. It is important to note that the targets were designed to constant layer count, and therefore have different target thicknesses and areal densities. The differences in target weights and thicknesses are important, and will be addressed in a follow-on study utilizing targets of constant total thickness and weight. Additional studies will formally quantify the flexibility of different fabric targets. However, the present targets are all thin and flexible, and of roughly similar weights and densities, so that their comparisons are still meaningful.

STF-fabrics provide better needle puncture resistance, most likely due to the decrease in yarn mobility. This observation is consistent with previous yarn pull-out and ballistic experiments (Egres et al., 2003; Decker et al., 2005). The STF acts to restrict motion of the filaments and yarns, preventing the sharp tip of the needle from pushing aside yarns and penetrating between them.

Unlike previous studies on needle puncture where a conical needle was used (Termonia, 2004), a hypodermic needle also cuts yarns while penetrating. The results show that STF treatments are effective against these multi-mode penetrators. This behavior is consistent with previous studies regarding quasistatic knife penetration of fabrics, which found that the addition of STF can increase the cutting resistance of Kevlar fabrics (Decker et al., 2007).

STF-779 performs better than STF-706 against small needle diameter threats. This behavior is due to the higher yarn count of 779, which restricts yarn mobility in a way analogous to the effects of adding STF to neat fabrics. However, due to the cutting edge of hypodermic needles, this effect does not carry over to larger needle diameters. At large needle diameters, cutting effects dominate windowing effects. In this damage mode, the heavier 706 fabric targets have more filaments per unit area than the 779 targets, providing a higher overall cut resistance. A systematic scaling study of needle gauge and yarn denier effects could be investigated in future studies.

It is interesting to note that testing of both STF and neat fabrics resulted in bent needles. The probabilistic needle bending behavior could be associated with the physical location at which the needle begins penetration. For example, a needle tip that starts penetration at the center of a yarn-yarn crossover might be more likely to bend than a needle tip that starts penetration between two yarns. Further investigation could be done to better analyze the needle bending phenomenon, and more quantitatively bound the probability of needle bending for different fabric and needle combinations.

In summary, the results show that STF-treatments can improve the hypodermic needle puncture resistance of fabrics while maintaining thinness and flexibility. These materials could find useful application in safety equipment for individuals that face the risk of needle contact, such as police officers and medical personnel.

5. REFERENCES

ASTM International Standard D4833-00e1 (2005).
H.A. Barnes, J. Rheol., 33, pp. 329-366 (1989).
J.W. Bender and N. J. Wagner, J. Colloid Interface Sci., 172, pp. 171-184 (1995).
G. Bossis and J.F. Brady, J. Chem. Phys., 91, pp. 1866-1874 (1989).
A.A. Catherall, J.R. Melrose, and R.C. Ball, J. Rheol., 44, pp. 1-25 (2000).
M.J. Decker, C.J. Halbach, C.H. Nam, N.J. Wagner, E.D. Wetzel, Comp Sci and Tech, 67, pp. 565-578 (2007).
M.J. Decker, R.G. Egres, E.D. Wetzel, and N.J. Wagner. Proceedings of the 22nd Int. Symp. on Ballistics, Vancouver, BC, Canada, (2005).
R.G. Egres Jr., Y.S. Lee, J.E. Kirkwood, K.M. Kirkwood, N.J. Wagner, and E.D. Wetzel, Proceedings, 14th Int. Conf. on Composite Materials, San Diego, CA, Soc. Manufacturing Engineers, paper #1513 (2003).
Y.S. Lee, E.D. Wetzel, R.G. Egres Jr, and N.J. Wagner, 23rd Army Science Conference, Orlando, FL, paper#A0-01 (2002).
Y.S. Lee, E.D. Wetzel, and N.J. Wagner, J. Mat. Sci., 38, pp. 2825-2833 (2003).
Y.S. Lee, and N.J. Wagner, Rheol. Acta, 42, pp. 199-208 (2003).
L.F. Leslie, J.A. Woods, J.G. Thacker, R.F. Morgan, W. McGregor, and R.F. Edlich, J. Biomed. Mater. Res. (Appl. Biomater.), 33, pp. 41-6 (1995).
B.J. Maranzano, and N.J. Wagner, J. Chem. Phys., 117, pp. 10291-10302 (2002).
B.J. Maranzano, and N.J. Wagner, J. Rheol., 45, pp. 1205-1222 (2001).
National Institute of Justice (NIJ) Standard 0115.00 (2000).
Y. Termonia, J. Imp. Eng., 32, pp. 1512-1520 (2006).